







RESEARCH ARTICLE | NOVEMBER 22 2023

Ultra-efficient machine learning design of nonreciprocal thermal absorber for arbitrary directional and spectral radiation

Zihe Chen ; Shilv Yu ; Cheng Yuan ; Kun Hu ; Run Hu  



J. Appl. Phys. 134, 203101 (2023)

<https://doi.org/10.1063/5.0177207>



View Online



Export Citation

CrossMark

AIP Advances

Why Publish With Us?

-  **25 DAYS**
average time to 1st decision
-  **740+ DOWNLOADS**
average per article
-  **INCLUSIVE**
scope

[Learn More](#)



Ultra-efficient machine learning design of nonreciprocal thermal absorber for arbitrary directional and spectral radiation

Cite as: J. Appl. Phys. 134, 203101 (2023); doi: 10.1063/5.0177207

Submitted: 20 September 2023 · Accepted: 5 November 2023 ·

Published Online: 22 November 2023



Zihe Chen,¹  Shilv Yu,¹  Cheng Yuan,²  Kun Hu,^{1,a)} and Run Hu^{1,a)} 

AFFILIATIONS

¹School of Energy and Power Engineering, Huazhong University of Science and Technology, Wuhan 430074, China

²Wuhan Fiberhome Fuhua Electric Co., Ltd, Wuhan 430074, China

Note: This paper is part of the special topic, Machine Learning for Thermal Transport.

a) Authors to whom correspondence should be addressed: hukun@hust.edu.cn and hurun@hust.edu.cn

ABSTRACT

Development of nanophotonics has made it possible to control the wavelength and direction of thermal radiation emission, but it is still limited by Kirchhoff's law. Magneto-optical materials or Weyl semimetals have been used in recent studies to break the time-reversal symmetry, resulting in a violation of Kirchhoff's law. Currently, most of the work relies on the traditional optical design basis and can only realize the nonreciprocal thermal radiation at a specific angle or wavelength. In this work, on the basis of material informatics, a design framework of a multilayer nonreciprocal thermal absorber with high absorptivity and low emissivity at any arbitrary wavelength and angle is proposed. Through a comprehensive investigation of the underlying mechanism, it has been discovered that the nonreciprocal thermal radiation effect is primarily attributed to excitation of the cavity mode at the interface between the metal and the multilayer structure. Moreover, the impact of factors, such as layer count, incidence angle, extinction coefficient, and applied magnetic field on nonreciprocal thermal radiation, is thoroughly explored, offering valuable insights to instruct the design process. Additionally, by expanding the optimization objective, it becomes feasible to design fixed dual-band or even multi-band nonreciprocal thermal absorbers. Consequently, this study offers essential guidelines for advancing the control of nonreciprocal thermal radiation.

22 November 2023 11:58:37

Published under an exclusive license by AIP Publishing. <https://doi.org/10.1063/5.0177207>

I. INTRODUCTION

With the advancement of photonic crystal technology, the potential to create emitters and absorbers with desired spectra and incident angles has become a reality.¹⁻³ Currently, most emitter/absorber designs adhere to Kirchhoff's law, which states that directional spectral emissivity equals directional spectral absorptivity for a specific polarization, wavelength, and incident angle.^{4,5} Consequently, when energy is absorbed by an object, a portion of it is inevitably returned to the emission source, resulting in inherent energy loss. However, Fan's pioneering research in 2014 showcased the possibility of breaking Kirchhoff's law, offering an exciting opportunity to enhance energy efficiency.⁶

Kirchhoff's law is a consequence of the Lorentz reciprocity theorem, which requires non-magnetic, stationary, and linear materials.^{7,8} Any violation of these conditions may upset this detail balance to achieve nonreciprocal thermal radiation. At present, in

the mid-infrared band range, the most common method to achieve nonreciprocity is by incorporating materials that break time-reversal symmetry into the design of the emitter/absorber, such as magneto-optical materials^{6,9-12} or magnetic Weyl semimetals.¹³⁻¹⁶ Among them, magneto-optical materials usually need a grating guide mode structure or a multilayer structure to strengthen the nonreciprocal effect because of weak nonreciprocity, which has been verified by corresponding experiments.¹⁷⁻¹⁹ Compared with the former, Weyl semimetal is an emerging magnetic material, although it shows excellent performance on nonreciprocal thermal radiation, but due to the immature preparation technology, it only stays in the design stage. In addition, considering the complex processing and preparation requirements of grating structures, it is challenging to implement them on a large scale. As a result, multilayer film structures with a simpler preparation process have garnered significant attention. However, the design of multilayer

nonreciprocal thermal emitters/absorbers involves several factors, including the number of layers, material used, thickness, incident angle, and so on, which increases the complexity of the design process. For instance, for an N -layer structure composed of two materials, there are 2^N possibilities to consider when accounting for only the number of layers, resulting in a significant challenge in manual optimization. As a result, most designs of nonreciprocal multilayer thermal emitters focus on ordered structures, such as photonic crystals^{11,20–22} or structures with specific sequences,^{23,24} which are far from reaching the design limit. Happily, with the development of machine learning, material informatics has been proven to have the ability to rapidly optimize structures and have been widely used in drug design,²⁵ interface thermal conductivity optimization,²⁶ thermal photovoltaic system design,²⁷ and so on. Therefore, exploring a more optimal design method for a multilayer nonreciprocal thermal emitter/absorber is the key to solving this problem.

In this work, we propose a design framework for a nonreciprocal thermal absorber with high absorptivity and low emissivity at a given wavelength and angle on the basis of material informatics. On this basis, the impact of factors, such as the number of layers, incidence angle, material parameters, and applied magnetic field, on nonreciprocal thermal radiation is explored. This comprehensive exploration offers valuable insights and provides a methodological foundation for the development of highly efficient and tailored nonreciprocal thermal absorbers.

II. METHODS

The nonreciprocal thermal absorber is composed of a multilayer structure with a metal aluminum layer at the bottom, in which the multilayer structure is composed of a magneto-optical material InAs and a dielectric material SiO₂. The layer number N of the multilayer structure is preliminarily set at 16. In addition, the refractive index of SiO₂ (n_1) is 1.45,^{11,28} and the dielectric constant of metal Al is calculated from the Drude model.²⁹ Breaking of the time-reversal symmetry requires an applied magnetic field along the y axis, which is taken as 3 T here. In this configuration, the magneto-optical material InAs has an asymmetric dielectric tensor, which is specifically expressed as^{6,29}

$$\boldsymbol{\epsilon} = \begin{bmatrix} \epsilon_{xx} & 0 & \epsilon_{xz} \\ 0 & \epsilon_{yy} & 0 \\ \epsilon_{zx} & 0 & \epsilon_{zz} \end{bmatrix}, \quad (1)$$

where

$$\epsilon_{xx} = \epsilon_{zz} = \epsilon_{\infty} - \frac{w_p^2(w + i\Gamma)}{w[(w + i\Gamma)^2 - w_c^2]}, \quad (2)$$

$$\epsilon_{yy} = \epsilon_{\infty} - \frac{w_p^2}{w(w + i\Gamma)}, \quad (3)$$

$$\epsilon_{xz} = -\epsilon_{zx} = i \frac{w_p^2 w_c}{w[(w + i\Gamma)^2 - w_c^2]}. \quad (4)$$

The parameters and definitions in the above formula can be found in Ref. 6. Here, the incident light is in the x - z plane with an

incident angle of θ , and only TM waves are considered. It is assumed that there is no transmission process present due to the presence of the bottom metal layer. Therefore, the calculation formulas for directional spectral emissivity $\epsilon(\lambda, \theta)$ and absorptivity $\alpha(\lambda, \theta)$ under the influence of a magnetic field are given by Eqs. (5) and (6), respectively,^{6,29}

$$\epsilon(\lambda, \theta) = 1 - R(\lambda, -\theta), \quad (5)$$

$$\alpha(\lambda, \theta) = 1 - R(\lambda, \theta). \quad (6)$$

Here, $R(\lambda, -\theta)$ and $R(\lambda, \theta)$ represent the directional reflection spectra at $-\theta$ and θ angles, respectively. Based on this, the transfer matrix method (TMM) is employed to calculate the corresponding directional absorption and emission spectra.²³

Considering a more optimized structural design, the Monte Carlo Tree Search algorithm is used to carry out structure design under the framework of material informatics, as shown in Fig. 1. The entire optimization design consists of five distinct stages: binary encoding, physical model construction, spectral calculation by TMM, objective evaluation, and feedback. Initially, the chosen material is assigned values of 0 and 1 to represent magneto-optical and dielectric materials, respectively. Leaf nodes are generated from the root node, and the selection of each node is evaluated by the parameter Upper Confidence Bound (UCB).³⁰ The higher the UCB value, the more likely it is to become a next leaf node. Second, the corresponding physical model is constructed for the generated sequence. Then, the absorptivity and emissivity spectra are calculated using TMM, and the optimization target is evaluated and fed back. Here, the optimization target $opt(loc_{opt}, \theta, \delta)$ is specifically expressed as

$$opt(loc_{opt}, \theta, \delta) = H(\delta - |loc_{opt} - loc_{peak}|) * |abs(loc_{peak}) - emi(loc_{peak})|, \quad (7)$$

where loc_{opt} is the target peak wavelength, loc_{peak} represents the calculated peak wavelength in the absorption spectrum of the corresponding absorber, $abs(loc_{peak})$ is the absorptivity at the calculated peak wavelength, $emi(loc_{peak})$ is the corresponding emissivity at the calculated peak wavelength, θ is the incident angle, and δ is the permissible fluctuation range of the calculated peak wavelength. The expression consists of two components. The former $H(\dots)$ is the Heaviside function that is used to select the peak wavelength. The latter is to control the degree of nonreciprocity, that is, the difference between the absorptivity and emissivity at the peak wavelength. The higher the product of these two components, the more optimized the structural design becomes.

III. RESULTS AND DISCUSSIONS

As shown in Fig. 1, the target peak wavelength (loc_{opt}) is set to 15 μm , and the corresponding material thicknesses of InAs and SiO₂ are set to $d_0 = \frac{loc_{opt}}{4 * \sqrt{|\epsilon_{xx}|}}$ and $d_1 = \frac{loc_{opt}}{4 * |n_1|}$, respectively. It should be noted that the thickness here represents the unit layer thickness. In addition, if there is no special indication, the number of layers N is 16 and the incidence angle is 50°. For the sequence

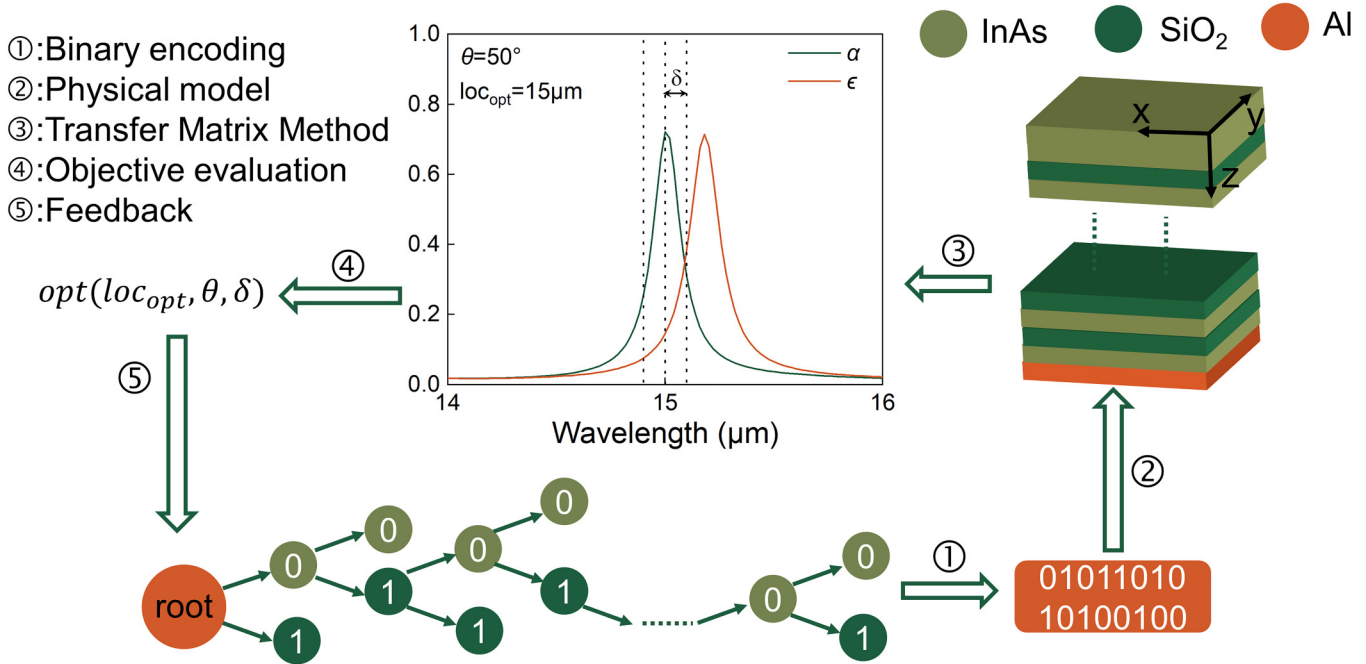


FIG. 1. The design framework of the nonreciprocal thermal absorber at fixed wavelength and angle based on machine learning.

01011010100100, the corresponding physical model is generated and the absorptivity and emissivity spectra are calculated by TMM. It can be seen that the absorptivity and emissivity spectra are obviously nonoverlapping, representing a violation of Kirchhoff's law. Here, for a 16-layer multilayer structure composed of two materials, the total possible results are 2^{16} , which is difficult for manual optimization. The method of machine learning can reduce the labor burden while evaluating the results after each calculation so that

the next iteration calculation can develop in a better direction. As shown in Fig. 2(a), the horizontal coordinate represents the percentage of the current cycles in the total cycles, while the vertical coordinate represents the optimization target value. Here, the total number of cycles is 9026. It can be seen that with only 4.099% iterative calculations, the target value opt can reach 0.907, which means that the difference between absorptivity and emissivity can reach 0.907 at the target peak wavelength of $15\mu m$ (fluctuation

22 November 2023 11:58:37

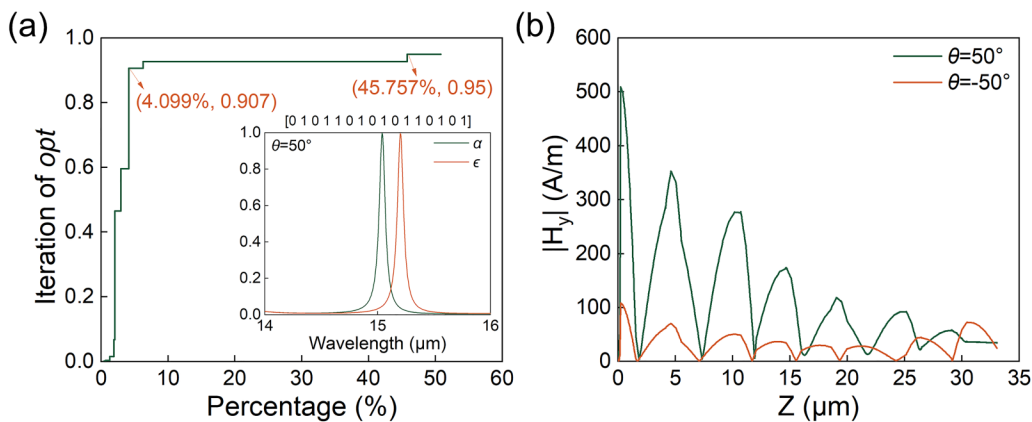


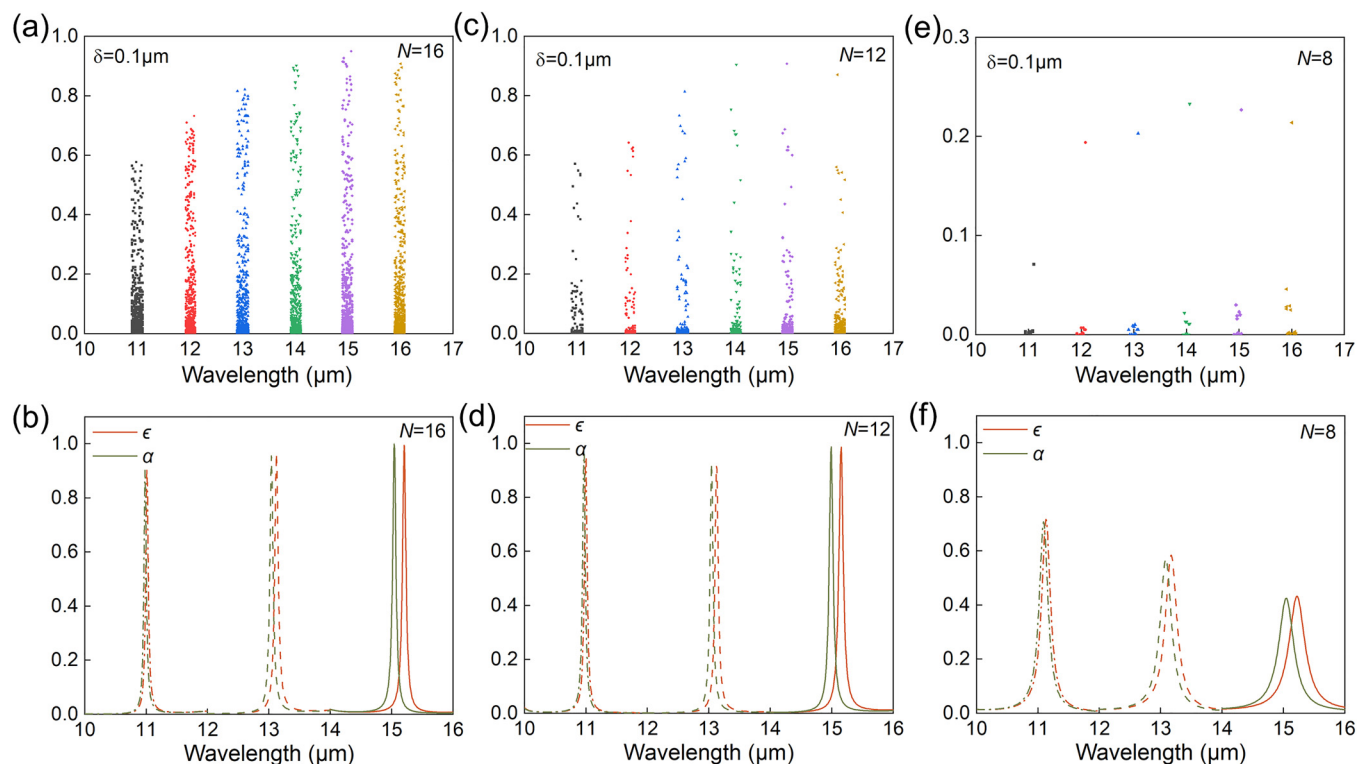
FIG. 2. (a) Tracing of opt vs iteration. (b) The magnetic field distribution $|H_y|$ along the z direction at a wavelength of $15.04\mu m$ at $\theta=50^\circ$ and $\theta=-50^\circ$ with $B=3 T$.

range δ is $0.1 \mu\text{m}$). This result demonstrates the high efficiency of the design method proposed in this study. Furthermore, the target value opt can reach 0.95 with 45.757% iterative calculations. At this point, the corresponding sequence is 0101101010110101, and the absorptivity and emissivity spectra are shown in the attached figure. It is notable that the absorptivity is close to 1 at a wavelength of $15.04 \mu\text{m}$, whereas the emissivity is only 0.048, indicating a strong nonreciprocity.

To better elucidate the underlying physical mechanism, magnetic field distribution at the wavelength of $15.04 \mu\text{m}$ is calculated, as shown in Fig. 2(b). When the incidence angle is 50° , the magnetic field amplitude has a large enhancement at the junction of the metal and the multilayer structure and gradually decreases along the distance from the metal. This phenomenon can primarily be attributed to the excitation of the cavity mode at the bottom interface between the magneto-optical material and the metal.³¹ The intensified magnetic field amplitude bolsters the absorption of photons by the structure, thereby imparting strong absorption characteristics to the entire system. Conversely, under an incident angle of -50° , the overall magnetic field amplitude appears small and relatively stable, indicating weak absorption of photons.

Next, to further validate the applicability of this design across different target peak wavelengths, the opt values have been statistically analyzed for various target wavelengths, as shown in Fig. 3(a).

It can be obviously seen that when the target peak wavelength is $11 \mu\text{m}$, the value of opt decreases significantly on the whole, and the maximum value is less than 0.6, which means that the degree of nonreciprocity is relatively weak at this wavelength. This is mainly because the degree of nonreciprocity is closely related to the value of $|\epsilon_{xz}/\epsilon_{xx}|$. When other parameters remain unchanged, the smaller the wavelength, the smaller the value of $|\epsilon_{xz}/\epsilon_{xx}|$, resulting in a weaker nonreciprocal effect. Additionally, the spectra corresponding to the optimal results at the target wavelengths of 11, 13, and $15 \mu\text{m}$ have been calculated, respectively, as shown in Fig. 3(b). It can be clearly seen that the optimized structure has a sharp peak at the corresponding target peak wavelength, but the degree of separation between the absorptivity and emissivity spectra is different. The larger the target wavelength, the greater the degree of nonreciprocity, which also corresponds to the statistical findings in Fig. 3(a). Here, the impact of layer N on nonreciprocity is also discussed, and the results are shown in Figs. 3(c)–3(f). On the one hand, as the number of layers decreases, the majority of opt values tend to concentrate in the lower region, indicating a decrease in the level of nonreciprocity. Especially, when the number of layers decreases to eight layers, the maximum opt value does not exceed 0.3. This can be attributed to the limited number of layers, which hinders efficient excitation of the cavity mode. On the other hand, it can be seen that when the number of layers is 12, the optimal



22 November 2023 11:58:37

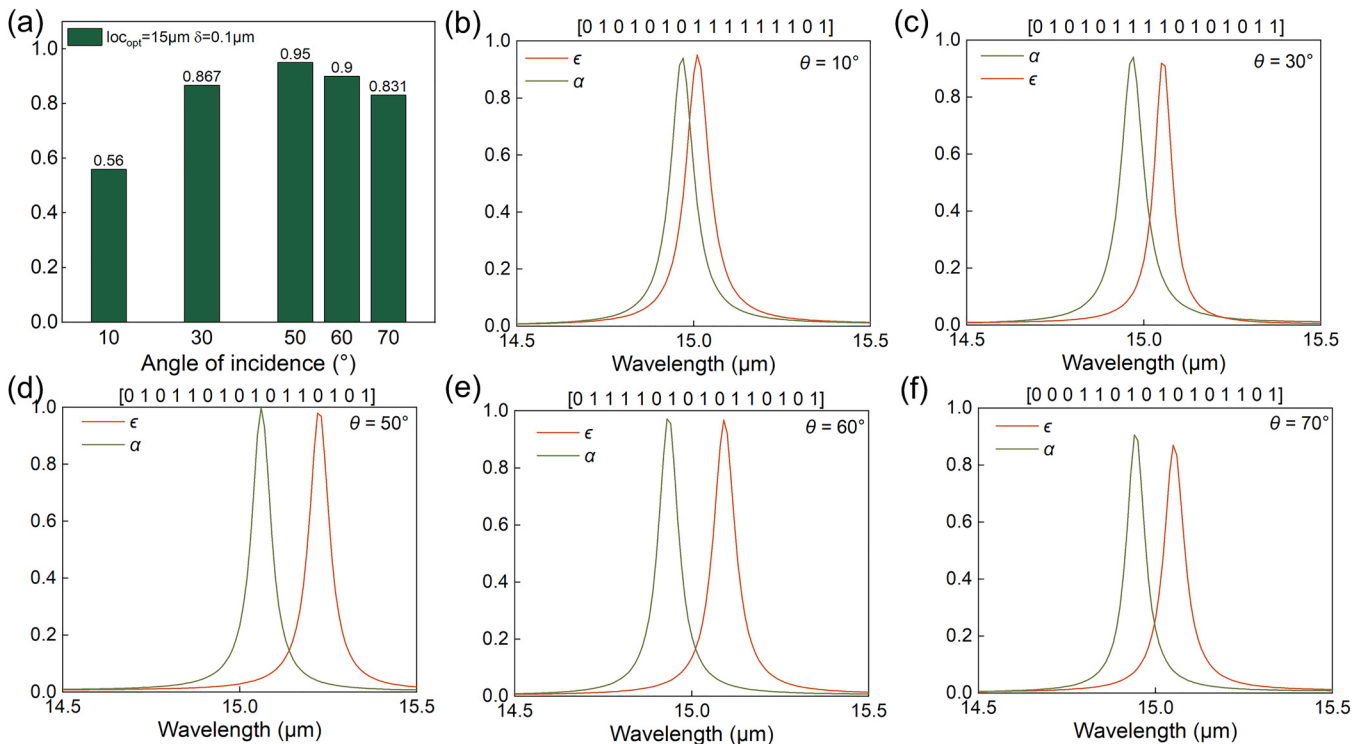
FIG. 3. Scatter distribution of target values (opt) at different target peak wavelengths with $\theta=50^\circ$: (a) $N=16$, (c) $N=12$, and (e) $N=8$. The absorptivity and emissivity spectra corresponding to the optimal opt value when the target peak wavelengths are 11, 13, and $15 \mu\text{m}$: (b) $N=16$, (d) $N=12$, and (f) $N=8$.

result can also achieve a strong nonreciprocity phenomenon, as shown in Fig. 3(d), which also means that there is no need to pursue more layers for better results. Therefore, by discussing the influence of the number of layers on nonreciprocity, it is better to guide the production practice.

Here, the effect of incident angle on the multilayer nonreciprocal thermal absorber is also explored based on the algorithm framework, and the *opt* values at 10°, 30°, 50°, 60°, and 70° are calculated, respectively. The values of optimal *opt* at various angles are shown in Fig. 4(a), and it is obvious that the optimal *opt* values first increase and then decrease as the incidence angle increases. When the incidence angle is reduced to 10°, the *opt* value is only 0.56, and the nonreciprocity is significantly reduced. This is mainly because the decreasing incidence angle weakens the effect of the asymmetric dielectric values (ϵ_{xz} and ϵ_{zx}), thus reducing the degree of deviation between the absorptivity and emissivity spectra, as shown in Fig. 4(b). As the incidence angle gradually increases to 70°, the nonreciprocity effect also shows a certain weakening. This is mainly because with the increase in the incidence angle, the reflection of the structure is significantly enhanced, which leads to the weakening of the absorption of the structure, as shown in Fig. 4(f). It can be obviously seen that the spectral peak value at an incident angle of 70° decreases as a whole, and, therefore, the

corresponding nonreciprocal effect is also weakened, compared with the spectra at the incident angles of 50° and 60°.

In practice, the refractive index of a dielectric material may contain an extinction coefficient (*k*). Through the investigation of the previous literature, it is found that the effect of an extinction coefficient on a multilayer nonreciprocal thermal absorber is rarely discussed. Here, based on the algorithm framework proposed in this work, the influence of different extinction coefficients on nonreciprocity is discussed. Initially, when the refractive index of the dielectric material $n_1 = 1.45 + 0.01i$ and other parameters remain unchanged, the optimal *opt* value is 0.728, as shown in Fig. 5(a). The sequence corresponding to the optimal result is 010000000101010, and its absorptivity and emissivity spectra are calculated, as shown in Fig. 5(b). It can be clearly seen that the nonreciprocity remains relatively strong. Then, consider further increasing the extinction coefficient to 0.05i or even 0.1i, as shown in Figs. 5(c)–5(f). It can be seen that a further increase in the extinction coefficient leads to a significant reduction in the degree of nonreciprocity. Especially, when the *k* value is 0.1i, the nonreciprocity of the optimized structure is only 0.08. Therefore, when constructing a nonreciprocal multilayer thermal emitter, dielectric materials should be selected with an extinction coefficient as small as possible.



22 November 2023 11:58:37

FIG. 4. (a) The optimal *opt* statistical graph at different incidence angles. The absorptivity and emissivity spectra corresponding to the optimal *opt* value at different incidence angles: (b) $\theta = 10^\circ$, (c) $\theta = 30^\circ$, (d) $\theta = 50^\circ$, (e) $\theta = 60^\circ$, and (f) $\theta = 70^\circ$.

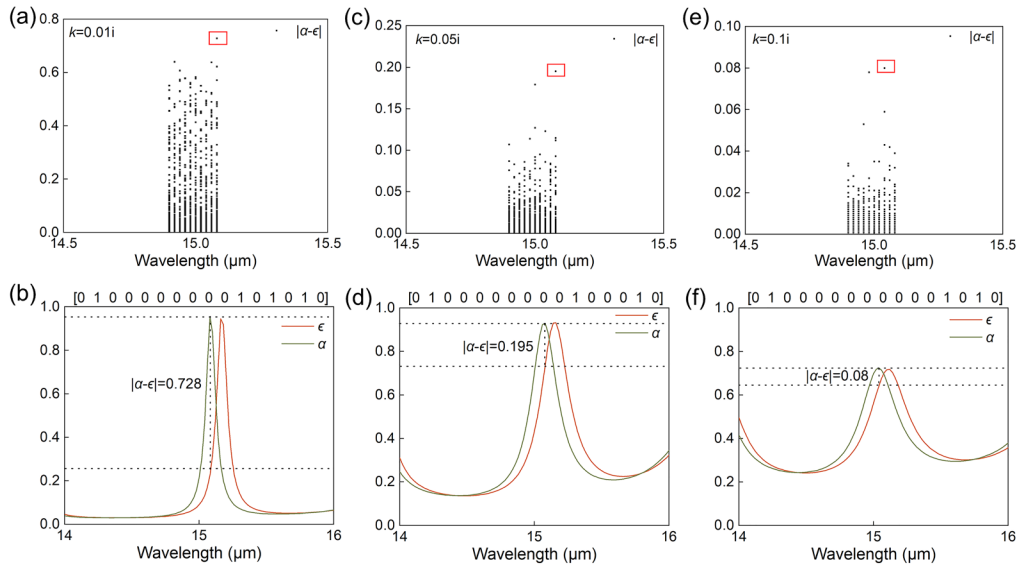


FIG. 5. The opt distribution map under different extinction coefficients: (a) $k=0.01i$, (c) $k=0.05i$, and (e) $k=0.1i$. The absorptivity and emissivity spectra corresponding to the optimal opt value under different extinction coefficients: (b) $k=0.01i$, (d) $k=0.05i$, and (f) $k=0.1i$.

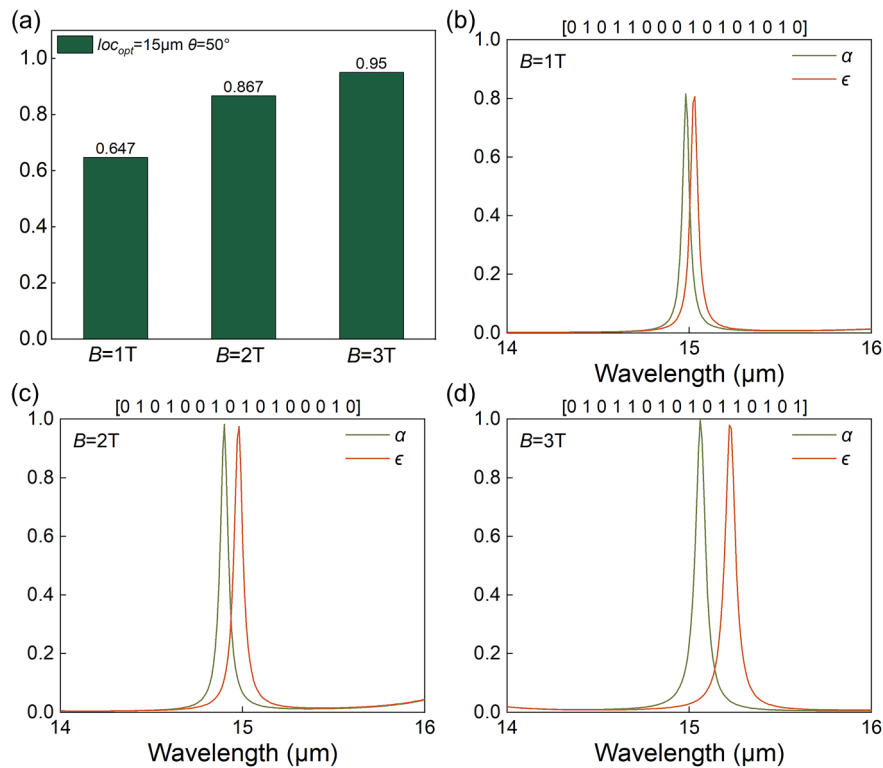


FIG. 6. (a) The statistical diagram of the optimal opt under different magnetic fields with $loc_{opt}=15\mu\text{m}$ and $\theta=50^\circ$. The absorptivity and emissivity spectra corresponding to the optimal opt value under different magnetic fields: (b) $B=1\text{T}$, (c) $B=2\text{T}$, and (d) $B=3\text{T}$.

22 November 2023 11:58:37

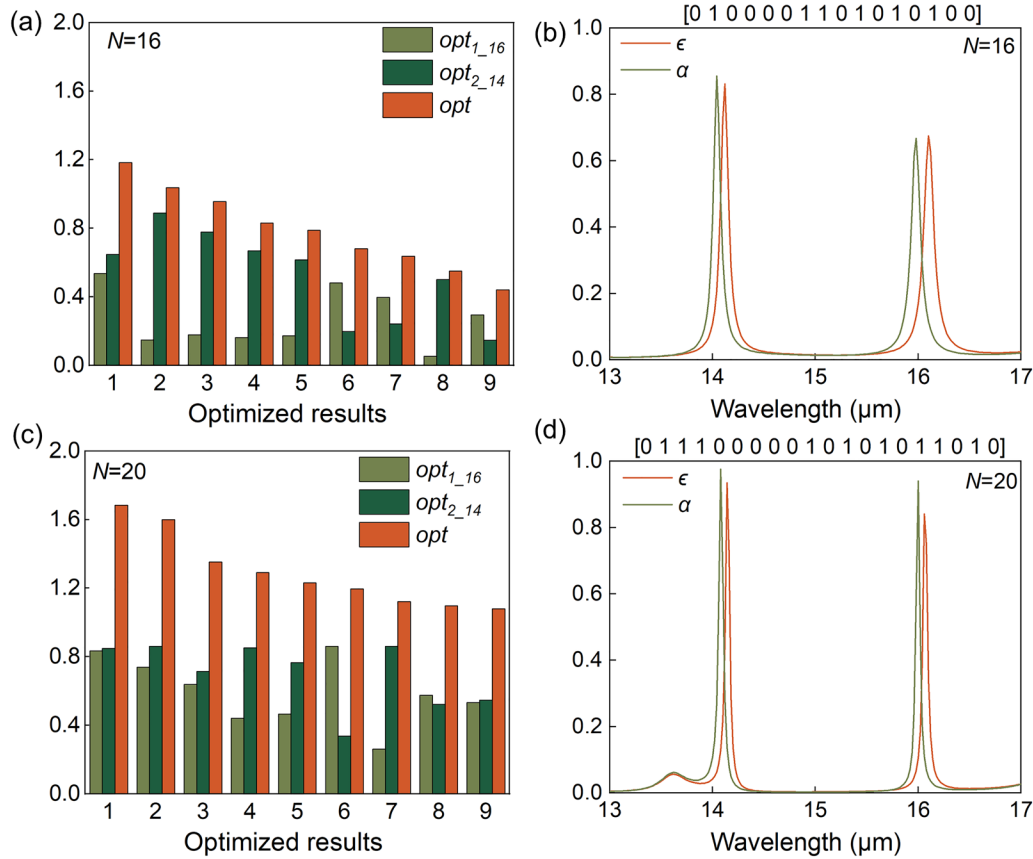


FIG. 7. The optimization results of different layer numbers under dual objective wavelength: (a) $N = 16$ and (c) $N = 20$. The absorptivity and emissivity spectra corresponding to the optimal opt value under different layers: (b) $N = 16$ and (d) $N = 20$.

22 November 2023 11:58:37

The effect of the magnetic field on nonreciprocal thermal radiation has been discussed when the target peak wavelength is $15\ \mu\text{m}$ and the incidence angle is 50° . As shown in Fig. 6(a), the optimal values under different magnetic fields are statistically analyzed. Among them, the optimal values under 1, 2, and 3 T are 0.647, 0.867, and 0.95, respectively. It is obvious that as the magnetic field decreases, the optimal values under different magnetic fields also decrease. This is because the nonreciprocity is mainly determined by the ratio of the asymmetric term ϵ_{xz} to the diagonal term ϵ_{xx} of the magneto-optical material's dielectric tensor. As the magnetic field decreases, this ratio also decreases, making the degree of nonreciprocity weaker. Figures 6(b)–6(d) are the spectral diagrams corresponding to the optimal results under 1, 2, and 3 T, respectively. It can also be seen that with the decrease in the magnetic field, the separation degree of the absorptivity and emissivity spectra is weakened, which means that the nonreciprocity is weakened.

Finally, to further supplement the algorithm framework, the multi-band optimization design is considered. Here, the target wavelengths $loc_{opt1} = 16\ \mu\text{m}$ and $loc_{opt2} = 14\ \mu\text{m}$ are taken as examples. The corresponding optimization targets are named opt_{1_16} and opt_{2_14} , respectively, and the final optimization target opt is the sum

of the two. In addition, the value of loc_{opt} is determined as $0.5(loc_{opt1} + loc_{opt2})$. When other conditions remain unchanged, the opt value is iteratively calculated and the top nine optimal results are selected to generate the corresponding bar chart, as shown in Fig. 7(a). At this point, the optimal opt value is 1.183, and the corresponding opt_{2_14} and opt_{1_16} values are 0.647 and 0.537, respectively. The sequence corresponding to the optimal result is 0100001101010100, and the associated absorptivity and emissivity spectra are illustrated in Fig. 7(b). Notably, it is evident that a certain nonreciprocity phenomenon is observed at the corresponding wavelengths of 14 and $16\ \mu\text{m}$, thereby highlighting the effectiveness of this design. In addition, considering increasing the number of layers N to 20 can enhance the nonreciprocal effect, and the optimization results are shown in Fig. 7(c). It is apparent that the opt value is larger compared to the case with 16 layers. This can be attributed to the fact that more layers facilitate the excitation of cavity mode resonance. The optimal opt value is 1.684, while the corresponding values for opt_{2_14} and opt_{1_16} are 0.848 and 0.835, respectively. The corresponding sequence is 01110000010101011010. The absorptivity and emissivity spectra presented in Fig. 7(d) exhibit a stronger nonreciprocal effect at the optimized target wavelength.

IV. CONCLUSION

In this work, a design framework of a multilayer nonreciprocal thermal absorber at an arbitrary angle and wavelength is proposed based on the Monte Carlo Tree Search algorithm, which greatly enhances the design process efficiency. By calculating the magnetic field distribution, it is found that the nonreciprocity is primarily attributed to the excitation of the cavity mode at the interface between the metal and the multilayer structure. Furthermore, the impacts of layer number, incident angle, extinction coefficient, and applied magnetic field on nonreciprocal thermal radiation are discussed. Moreover, by further supplementing the target value, the design of dual-band nonreciprocal thermal radiation can also be well realized. The realization of this work provides a guiding basis for the design of multilayer nonreciprocal thermal absorbers/emitters.

ACKNOWLEDGMENTS

The authors would like to acknowledge the financial support by the National Natural Science Foundation of China (NNSFC) (Nos. 52211540005 and 52076087), the Natural Science Foundation of Hubei Province (No. 2023AFA072), the National Key R & D Project from Ministry of Science and Technology of China (No. 2022YFA1203100), the Open Project Program of Wuhan National Laboratory for Optoelectronics (No. 2021WNLOKF004), Wuhan Knowledge Innovation Shuguang Program, and the Science and Technology Program of Hubei Province (No. 2021BLB176).

AUTHOR DECLARATIONS

Conflict of Interest

The authors have no conflicts to disclose.

Author Contributions

Zihe Chen: Conceptualization (equal); Data curation (equal); Formal analysis (equal); Methodology (equal); Validation (equal); Writing – original draft (equal); Writing – review & editing (equal). **Shilv Yu:** Formal analysis (equal); Methodology (equal); Writing – review & editing (equal). **Cheng Yuan:** Writing – review & editing (equal). **Kun Hu:** Formal analysis (equal); Supervision (equal); Writing – review & editing (equal). **Run Hu:** Conceptualization (equal); Formal analysis (equal); Supervision (equal); Writing – original draft (equal); Writing – review & editing (equal).

DATA AVAILABILITY

The data that support the findings of this study are available from the corresponding authors upon reasonable request.

REFERENCES

- ¹J.-W. Cho, Y.-J. Lee, J.-H. Kim, R. Hu, E. Lee, and S.-K. Kim, “Directional radiative cooling via exceptional epsilon-based microcavities,” *ACS Nano* **17**(11), 10442–10451 (2023).
- ²J. S. Hwang, J. Xu, and A. P. Raman, “Simultaneous control of spectral and directional emissivity with gradient epsilon-near-zero InAs photonic structures,” *Adv. Mater.* **35**(39), 2302956 (2023).

- ³J. Yu, R. Qin, Y. Ying, M. Qiu, and Q. Li, “Asymmetric directional control of thermal emission,” *Adv. Mater.* **35**, e2302478 (2023).
- ⁴G. I. Kirchhoff, “On the relation between the radiating and absorbing powers of different bodies for light and heat,” *London Edinburgh Dublin Philos. Mag. J. Sci.* **20**, 1–21 (1860).
- ⁵Z. M. Zhang, X. Wu, and C. Fu, “Validity of Kirchhoff’s law for semitransparent films made of anisotropic materials,” *J. Quant. Spectrosc. Radiat. Transfer* **245**, 106904 (2020).
- ⁶L. Zhu and S. Fan, “Near-complete violation of detailed balance in thermal radiation,” *Phys. Rev. B* **90**(22), 220301 (2014).
- ⁷M. Q. Liu and C. Y. Zhao, “Near-infrared nonreciprocal thermal emitters induced by asymmetric embedded eigenstates,” *Int. J. Heat Mass Transfer* **186**, 122435 (2022).
- ⁸S. E. Han, “Theory of thermal emission from periodic structures,” *Phys. Rev. B* **80**(15), 155108 (2009).
- ⁹J. Wu, F. Wu, and X. Wu, “Strong dual-band nonreciprocal radiation based on a four-part periodic metal grating,” *Opt. Mater.* **120**, 111476 (2021).
- ¹⁰X. Wu, R. Liu, H. Yu, and B. Wu, “Strong nonreciprocal radiation in magnetophotonic crystals,” *J. Quant. Spectrosc. Radiat. Transfer* **272**, 107794 (2021).
- ¹¹J. Wu, F. Wu, T. Zhao, M. Antezza, and X. Wu, “Dual-band nonreciprocal thermal radiation by coupling optical Tamm states in magnetophotonic multilayers,” *Int. J. Therm. Sci.* **175**, 107457 (2022).
- ¹²Z. Chen, S. Yu, B. Hu, and R. Hu, “Multi-band and wide-angle nonreciprocal thermal radiation,” *Int. J. Heat Mass Transfer* **209**, 124149 (2023).
- ¹³B. Zhao, C. Guo, C. A. C. Garcia, P. Narang, and S. Fan, “Axion-field-enabled nonreciprocal thermal radiation in Weyl semimetals,” *Nano Lett.* **20**(3), 1923–1927 (2020).
- ¹⁴S. Pajovic, Y. Tsurimaki, X. Qian, and G. Chen, “Intrinsic nonreciprocal reflection and violation of Kirchhoff’s law of radiation in planar type-I magnetic Weyl semimetal surfaces,” *Phys. Rev. B* **102**(16), 165417 (2020).
- ¹⁵J. Wu, Z. Wang, H. Zhai, Z. Shi, X. Wu, and F. Wu, “Near-complete violation of Kirchhoff’s law of thermal radiation in ultrathin magnetic Weyl semimetal films,” *Opt. Mater. Express* **11**(12), 4058–4066 (2021).
- ¹⁶J. Wu, B. Wu, Z. Wang, and X. Wu, “Strong nonreciprocal thermal radiation in Weyl semimetal-dielectric multilayer structure,” *Int. J. Therm. Sci.* **181**, 107788 (2022).
- ¹⁷K. J. Shayegan, B. Zhao, Y. Kim, S. Fan, and H. A. Atwater, “Nonreciprocal infrared absorption via resonant magneto-optical coupling to InAs,” *Sci. Adv.* **8**, eabm4308 (2022).
- ¹⁸K. J. Shayegan, S. Biswas, B. Zhao, S. Fan, and H. A. Atwater, “Direct observation of the violation of Kirchhoff’s law of thermal radiation,” *Nat. Photonics* **17**, 891–896 (2023).
- ¹⁹M. Liu, S. Xia, W. Wan, J. Qin, H. Li, C. Zhao, L. Bi, and C.-W. Qiu, “Broadband mid-infrared non-reciprocal absorption using magnetized gradient epsilon-near-zero thin films,” *Nat. Mater.* **22**, 1196–1202 (2023).
- ²⁰J. Wu, Y. Sun, F. Wu, B. Wu, and X. Wu, “Enhancing nonreciprocal thermal radiation in Weyl semimetals based on optical Tamm states by integrating with photonic crystals,” *Waves Random Complex Media* (to be published).
- ²¹M. Luo and Y. Xiao, “Strong nonreciprocal thermal radiation based on topological edge state in one-dimensional photonic crystal with Weyl semimetal,” *Int. J. Heat Mass Transfer* **211**, 124259 (2023).
- ²²J. Wu, H. Li, C. Fu, and X. Wu, “High quality factor nonreciprocal thermal radiation in a weyl semimetal film via the strong coupling between tamm plasmon and defect mode,” *Int. J. Therm. Sci.* **184**, 107902 (2023).
- ²³J. Wu, Z. Wang, B. Wu, Z. Shi, and X. Wu, “The giant enhancement of nonreciprocal radiation in Thue-morse aperiodic structures,” *Opt. Laser Technol.* **152**, 108138 (2022).
- ²⁴J. Wu and Y. M. Qing, “A multi-band nonreciprocal thermal emitter involving a Weyl semimetal with a Thue-Morse multilayer,” *Phys. Chem. Chem. Phys.* **25**(16), 11477–11483 (2023).
- ²⁵D. Wishart, “Bioinformatics in drug development and assessment,” *Drug Metab. Rev.* **37**(2), 279–310 (2005).

- ²⁶S. Ju, T. Shiga, L. Feng, Z. Hou, K. Tsuda, and J. Shiomi, “Designing nanostructures for phonon transport via Bayesian optimization,” *Phys. Rev. X* **7**(2), 021024 (2017).
- ²⁷R. Hu, J. Song, Y. Liu, W. Xi, Y. Zhao, X. Yu, Q. Cheng, G. Tao, and X. Luo, “Machine learning-optimized Tamm emitter for high-performance thermophotovoltaic system with detailed balance analysis,” *Nano Energy* **72**, 104687 (2020).
- ²⁸E. Palik, *Handbook of Optical Constants of Solids* (Academic, 1998).
- ²⁹B. Zhao, Y. Shi, J. Wang, Z. Zhao, N. Zhao, and S. Fan, “Near-complete violation of Kirchhoff’s law of thermal radiation with a 0.3 T magnetic field,” *Opt. Lett.* **44**(17), 4203–4206 (2019).
- ³⁰W. Xi, Y. Liu, J. Song, R. Hu, and X. Luo, “High-throughput screening of a high-Q mid-infrared Tamm emitter by material informatics,” *Opt. Lett.* **46**(4), 888–891 (2021).
- ³¹J. Wu and Y. M. Qing, “Strong nonreciprocal radiation with topological photonic crystal heterostructure,” *Appl. Phys. Lett.* **121**(11), 112201 (2022).